Why is the Aero Space So Loud? A Numerical Simulation of Sound Wave Propagation via FDTD Methods

Golemis, Shaun [*] , Kemp, John [†] , Ochs, Ben [‡] , Peters, Karsten [§] , and Veranga, Joshua [¶]
University of Illinois at Urbana-Champaign, Champaign, IL 61801, USA

This project presents a numerical simulation of acoustic wave propagation in a two-dimensional reflective environment using an explicit second-order finite-difference time-domain (FDTD) scheme. A speech-like waveform is introduced as a time-varying source, and its interaction with room geometry—including rigid walls and rectangular pillars—is analyzed. The study verifies the numerical method through convergence testing and applies it to increasingly complex scenarios, from symmetric box domains to realistic room layouts modeled after the UIUC Aerospace lounge, the "Aero Space". Results demonstrate how reflections, diffraction, and interference contribute to standing wave formation and localized pressure amplification. These findings highlight the capability of FDTD methods to model real-world acoustic behavior in enclosed reflective spaces.

I. Nomenclature

$u(x, y, t)$	=	Acoustic pressure deviation from equilibrium, Pa
c	=	Speed of sound in air, m/s
f_k	=	Central frequency of the k-th syllable, Hz
t_k	=	Temporal center of the k-th syllable, s
β_k	=	Width parameter (spread) of the k-th syllable, s^{-2}
A_k	=	Amplitude of the k-th speech pulse, dimensionless
$s(t)$	=	Time-varying speech source waveform, dimensionless
$s_k(t)$	=	Individual pulse for k-th syllable, dimensionless
i, j	=	Spatial grid indices in x and y
n	=	Time step index
$x_i = i\Delta x$	=	Discretized x-position, m
$y_j = j\Delta y$	=	Discretized y-position, m
$t^n = n\Delta t$	=	Discretized time, s
Δx	=	Grid spacing in x, m
Δy	=	Grid spacing in y, m
Δt	=	Time step, s
N_x, N_y	=	Number of grid points in x and y
N_t	=	Total number of time steps
L_x, L_y	=	Domain dimensions in x and y, m
$\nabla^2 u$	=	Discrete Laplacian of pressure field, Pa/m^2
ε	=	Grid-2 (discrete L^2) error norm, Pa
α	=	Gaussian width coefficient in manufactured solution, m^{-2}

[*]BS Student, Aerospace Engineering, Grainger College of Engineering, 104 S Wright St, Urbana, Illinois 61820, golemis2@illinois.edu
[†]BS Student, Aerospace Engineering, Grainger College of Engineering, 104 S Wright St, Urbana, Illinois 61820, jwkemp2@illinois.edu
[‡]BS Student, Aerospace Engineering, Grainger College of Engineering, 104 S Wright St, Urbana, Illinois 61820, bochs2@illinois.edu
[§]BS Student, Aerospace Engineering, Grainger College of Engineering, 104 S Wright St, Urbana, Illinois 61820, kjp@illinois.edu
[¶]BS Student, Aerospace Engineering, Grainger College of Engineering, 104 S Wright St, Urbana, Illinois 61820, veranga2@illinois.edu

ω	=	Temporal frequency in manufactured solution, rad/s
$\partial\Omega$	=	Domain boundary and obstacle surfaces
CFL	=	Courant–Friedrichs–Lewy number
$u_{i,j}^n$	=	Approximation to $u(x_i, y_j, t^n)$, Pa
i_0, j_0	=	Indices of the source location in the grid
$f(x, y)$	=	Initial pressure distribution, Pa
$g(x, y)$	=	Initial velocity distribution $\frac{\partial u}{\partial t}(x, y, 0)$, Pa/s

II. Introduction

Accurately modeling acoustic wave propagation in reflective environments is essential for a range of engineering applications, including aerospace vehicle design, architectural acoustics, and audio system development. This project investigates acoustic behavior in enclosed spaces using a second-order accurate finite-difference time-domain (FDTD) scheme to solve the two-dimensional wave equation. A time-varying speech-like waveform is introduced as an acoustic source to examine how realistic audio signals interact with complex boundaries.

The primary objective is to assess how pressure waves propagate, reflect, and interfere within a room geometry that includes rigid walls and internal rectangular pillars. Specifically, the study explores three questions: how do waves reflect and interfere in a bounded reflective room; what qualitative effects do internal obstacles introduce; and can standing wave behavior be captured and visualized using synthetic speech inputs. The simulation results aim to provide insight into why mostly reflective rooms, such as the UIUC Aero Space, can subjectively appear acoustically "loud" even with sparse conversational activity.

III. Mathematical Formulation

We aim to numerically solve the two-dimensional acoustic wave equation, which governs the propagation of pressure fluctuations in a homogeneous, inviscid medium. The respective equation is expressed as:

$$\frac{\partial^2 u}{\partial t^2} = c^2 \left(\frac{\partial^2 u}{\partial x^2} + \frac{\partial^2 u}{\partial y^2} \right), \tag{1}$$

where $u(x, y, t)$ is the acoustic pressure deviation from equilibrium and c is the speed of sound in air. This formulation is standard for the linearized 2D acoustic wave equation and serves as a model for time-domain numerical simulations in both acoustics and electrodynamics [1, 2].

A. Spatial and Temporal Discretization

We define a uniform Cartesian grid over the domain, with:

$$x_i = i\Delta x, \quad y_j = j\Delta y, \quad t^n = n\Delta t,$$

where $i, j, n \in \mathbb{Z}$ and denote the numerical approximation at grid point (i, j) and time step n as:

$$u_{i,j}^n \approx u(x_i, y_j, t^n).$$

To approximate the spatial and temporal second derivatives in the wave equation (1), we apply second-order central differences:

$$\frac{\partial^2 u}{\partial t^2} \approx \frac{u_{i,j}^{n+1} - 2u_{i,j}^n + u_{i,j}^{n-1}}{\Delta t^2}, \tag{2}$$

$$\frac{\partial^2 u}{\partial x^2} \approx \frac{u_{i+1,j}^n - 2u_{i,j}^n + u_{i-1,j}^n}{\Delta x^2}, \tag{3}$$

$$\frac{\partial^2 u}{\partial y^2} \approx \frac{u_{i,j+1}^n - 2u_{i,j}^n + u_{i,j-1}^n}{\Delta y^2}. \tag{4}$$

Substituting these finite difference approximations into the wave equation yields the fully discrete update formula:

$$\frac{u_{i,j}^{n+1} - 2u_{i,j}^{n} + u_{i,j}^{n-1}}{\Delta t^2} = c^2 \left(\frac{u_{i+1,j}^{n} - 2u_{i,j}^{n} + u_{i-1,j}^{n}}{\Delta x^2} + \frac{u_{i,j+1}^{n} - 2u_{i,j}^{n} + u_{i,j-1}^{n}}{\Delta y^2} \right). \tag{5}$$

Multiplying both sides by Δt^2 and solving for $u_{i,j}^{n+1}$ gives the final definition of the time-marching update rule:

$$u_{i,j}^{n+1} = 2u_{i,j}^{n} - u_{i,j}^{n-1} + c^2 \Delta t^2 \left(\frac{u_{i+1,j}^{n} - 2u_{i,j}^{n} + u_{i-1,j}^{n}}{\Delta x^2} + \frac{u_{i,j+1}^{n} - 2u_{i,j}^{n} + u_{i,j-1}^{n}}{\Delta y^2} \right). \tag{6}$$

This explicit finite-difference time-domain (FDTD) method allows for the advancement of the solution in time using known values at the current and previous time levels. This explicit update structure is a classical second-order FDTD scheme and is widely used for solving wave propagation problems in structured grids [1, 2].

B. Boundary and Initial Conditions

We enforce homogeneous Dirichlet boundary conditions throughout the domain expressed as

$$u_{i,j}^{n} = 0 \quad \text{for all } (i, j) \in \partial\Omega, \tag{7}$$

where $\partial\Omega$ includes both the outer boundaries (walls) and interior obstacles (pillars) of the room. In implementation, this is enforced by masking these points and resetting them to zero after each time step.

To initiate the scheme, two time steps are required. These are defined using:

$$u_{i,j}^{0} = f(x_i, y_j), \tag{8}$$

$$u_{i,j}^{-1} = f(x_i, y_j) - \Delta t \cdot g(x_i, y_j), \tag{9}$$

where $f(x, y)$ is the initial pressure distribution and $g(x, y) = \frac{\partial u}{\partial t}(x, y, 0)$ is the initial velocity field. In our simulations, we assume the medium is initially at rest, so $g = 0$, leading to $u^{-1} = u^{0}$.

C. Stability Analysis

This explicit time-stepping scheme is only stable if the Courant–Friedrichs–Lewy (CFL) condition is satisfied. For the two-dimensional wave equation, this condition takes the form:

$$\Delta t \leq \frac{1}{c} \left(\frac{1}{\Delta x^2} + \frac{1}{\Delta y^2} \right)^{-1/2}. \tag{10}$$

This criterion ensures that information does not propagate faster than the numerical scheme can resolve, preserving causality and preventing divergence of the solution. We enforce this condition in code by computing the maximum allowable time step based on the spatial discretization and setting Δt accordingly.

IV. Numerical Implementation

The numerical scheme described above was implemented in Python to simulate wave propagation in a two-dimensional domain. This section outlines the core components of the solver and their alignment with the FDTD formulation.

A. Domain and Discretization

The spatial domain of the defined room is a rectangular region measuring approximately $L_x = 15$ m in length and $L_y = 5$ m in width. In our respective simulation, it is discretized into a uniform Cartesian grid of $N_x = 601$ and $N_y = 201$ points, leading to grid spacings of $\Delta x = 0.025$ m and $\Delta y = 0.025$ m. The temporal resolution is governed by the CFL condition from Eq.(10), expressed as

$$\Delta t = \text{CFL} \cdot \frac{\min(\Delta x, \Delta y)}{c}, \tag{11}$$

with chosen values of CFL = 0.4 and $c = 343$ m/s. These values ensure numerical stability throughout the simulation.

The simulation is initialized with a quiescent medium—zero pressure and zero initial velocity—which corresponds to the initial conditions:

$$u^0_{i,j} = 0, \tag{12}$$

$$u^{-1}_{i,j} = 0, \tag{13}$$

for all interior grid points. These two time levels are required to begin the explicit time-marching scheme, with a total of N_t time steps computed to cover the simulation window of $T = 0.05$ s, where $N_t = T/\Delta t$.

B. Interior Masking and Boundary Conditions

The domain follows the layout of a plane defined by the layout of the Aero Space* at an approximate speaking height of 1.65 m. At this height, it includes internal obstacles of pillars—ignoring the other obstacles of tables and chairs as they're below the simulated height—and irregular wall segments following the shape of the room. These are encoded using a binary mask, constructed via polygonal definitions from the `shapely` library. This mask is used to:

- Apply homogeneous Dirichlet boundary conditions ($u = 0$) at wall and obstacle surfaces,
- Exclude non-interior points from the FDTD update rule,
- Reset masked values to zero after each time step.

This approach enables the modeling of complex geometries of wave propagation without altering the structured grid [3].

C. Time-Stepping Algorithm

The FDTD update rule is applied using three 2D arrays to store u^{n-1}, u^n, and u^{n+1}. At each time step, the following operations are performed:

1) Compute the discrete Laplacian of u^n using second-order central differences:

$$\nabla^2 u^n_{i,j} \approx \frac{u^n_{i+1,j} - 2u^n_{i,j} + u^n_{i-1,j}}{\Delta x^2} + \frac{u^n_{i,j+1} - 2u^n_{i,j} + u^n_{i,j-1}}{\Delta y^2}.$$

2) Advance the solution in time using the FDTD update:

$$u^{n+1}_{i,j} = 2u^n_{i,j} - u^{n-1}_{i,j} + c^2 \Delta t^2 \nabla^2 u^n_{i,j}.$$

3) Add the source term at a specified location (i_0, j_0):

$$u^{n+1}_{i_0,j_0} \mathrel{+}= s(t^n),$$

where $s(t)$ is the normalized speech waveform sampled at time t^n.

4) Enforce boundary conditions by zeroing all values at masked (non-interior) locations.

The corresponding Python snippet for the aforementioned follows this logic:

```
laplacian = ((roll(u_n, 1, axis=0) - 2*u_n + roll(u_n, -1, axis=0)) / dx**2
           + (roll(u_n, 1, axis=1) - 2*u_n + roll(u_n, -1, axis=1)) / dy**2)

u_np1[interior] = 2*u_n[interior] - u_nm1[interior] + c**2 * dt**2 * laplacian[interior]
u_np1[i0, j0] += signal[n]
u_np1[~interior] = 0
```

D. Source Implementation

The source term is implemented as a time-varying pressure input added at a fixed spatial location (i_0, j_0) which lies within the interior of the domain. This models a localized acoustic emitter, such as a human speaker.

The waveform $s(t)$ represents a simplified approximation of human speech, modeled as a series of three overlapping pulses corresponding to the syllables from the phrase "Hello there" ("heh," "lo," and " there"). Each pulse is generated using a modulated sinusoid of the form:

$$s_k(t) = A_k \sin(2\pi f_k t) \cdot \exp\left(-\beta_k (t - t_k)^2\right), \tag{14}$$

*Located on the second floor of Talbot Laboratory, 104 S. Wright St. Urbana, IL 61801

where f_k is the central frequency of the k-th syllable, t_k is its temporal center, β_k controls the duration (spread), and A_k is the amplitude. The complete speech signal is constructed by summing three such pulses:

$$s(t) = s_1(t) + s_2(t) + s_3(t), \tag{15}$$

with approximate central frequencies chosen as:

$$\begin{cases} f_1 = 250 \text{ Hz} & \text{“heh”}, \\ f_2 = 300 \text{ Hz} & \text{“lo”}, \\ f_3 = 275 \text{ Hz} & \text{“there”}. \end{cases}$$

Each pulse is temporally offset by approximately 10–15 milliseconds from the previous one to mimic the natural cadence of speech. And to ensure numerical stability and physical realism, the combined waveform is normalized such that:

$$\max_t |s(t)| = 1. \tag{16}$$

This avoids the introduction of excessively large pressure gradients that could destabilize the simulation or produce nonphysical results.

The signal is precomputed and stored as a one-dimensional array. During the simulation, the value $s(t^n)$ is added to $u^{n+1}_{i_0,j_0}$ at each time step t^n. This direct injection acts as an external forcing term and initiates wave propagation into the domain as a time-varying source implemented as an additive pressure term at a single grid point. The waveform $s(t)$ is precomputed from an audio sample and normalized in amplitude to avoid numerical instability. It is injected directly into the pressure field, modeling a localized acoustic source such as a speaker or human voice.

E. Data Output and Visualization

Snapshots of the pressure field are saved at specified intervals for postprocessing. Visualizations include contour plots of $u(x, y, t)$ at selected times, showing wave propagation, reflection, diffraction, and interference patterns. Additionally, animations are generated using `matplotlib.animation` to depict the full time evolution.

V. Results and Discussion

This section presents both the numerical verification of the method and the results of increasingly complex acoustic simulations. The structure follows a logical progression: we first confirm that the solver achieves the expected convergence behavior, then explore wave dynamics in geometries of increasing complexity—from simple rectangular boxes to the realistic room environment with internal obstacles and multiple sources.

A. Convergence Study

To validate the accuracy of the numerical scheme, we performed a grid refinement study using the manufactured solution:

$$u(x, y, t) = \exp\left(-\alpha[(x - x_0)^2 + (y - y_0)^2]\right) \cos(\omega t),$$

where α and ω are constants that ensure the solution remains smooth and bounded over time. The simulation was run for multiple grid resolutions, and the L^2 error norm was computed against the exact solution:

$$\varepsilon = \left(\sum_{i,j} \left(u^{\text{num}}_{i,j} - u^{\text{exact}}_{i,j} \right)^2 \Delta x \Delta y \right)^{1/2}.$$

Figure 1 shows a log-log plot of error versus grid spacing Δx. The observed slope of the error curve matches the expected second-order convergence rate of the FDTD method. This confirms that the implementation is consistent and accurate, providing a solid foundation for the physical simulations that follow.

The simulation parameters vital to accurately studying the acoustics were the grid spacing of the room and the time step size. The chosen values for those parameters are described in Section IV.A.

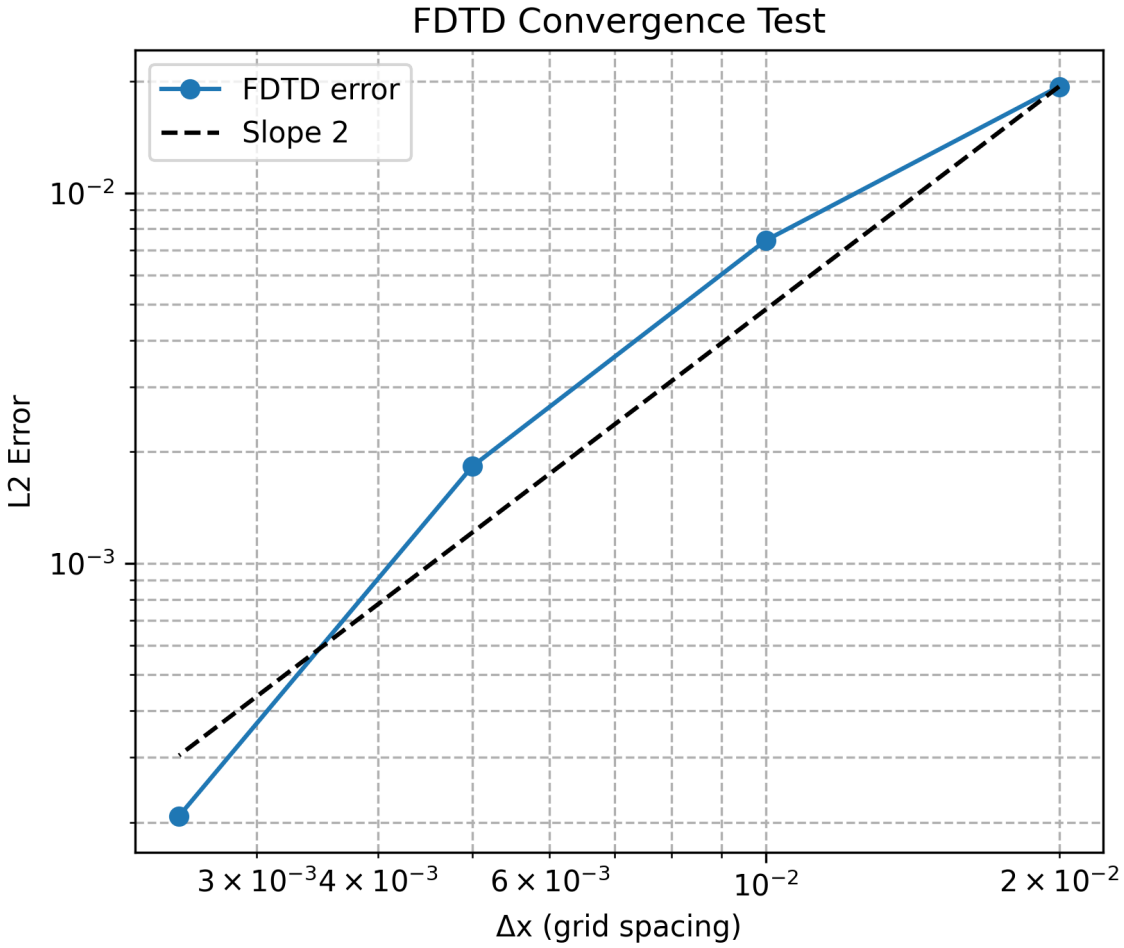

Fig. 1 Log-log plot of the L^2 error versus grid spacing Δx for the FDTD solver, using a manufactured analytical solution.

B. Pulse Propagation in a Simple Box

Figure 3 shows the evolution of a single acoustic pulse emitted from the center of a rectangular box with reflective boundaries. The wavefront maintains circular symmetry as it expands, and reflections from the walls occur at times and positions consistent with the wave speed c. This test serves as a baseline verification case and demonstrates that the numerical scheme respects geometric symmetry and conserves energy in the absence of internal obstacles.

C. Speech-Like Source in a Box

In Figure 4, a stylized speech waveform—composed of three consecutive pulses representing the syllables "heh," "lo," and "there"—is emitted from the same central location. The superposition of pulses results in more intricate wavefields, with visible regions of constructive and destructive interference. Despite the added source complexity, the overall symmetry is retained due to the simple geometry. This confirms that the solver can robustly handle overlapping signals and pressure buildup within a bounded domain.

D. Pulse in a Room with Obstacles

Figure 5 depicts the propagation of a single pulse in a more realistic room environment modeled after the UIUC Aero Space. The domain includes internal rectangular pillars and nonuniform boundary geometry. As the wavefront interacts with these features, it becomes distorted and asymmetric. Diffraction effects are especially pronounced around the pillars, and reflected wavefronts generate complex interference patterns throughout the room. This result demonstrates how geometric complexity breaks symmetry and significantly alters wave behavior, even for a simple pulse input.

E. Speech in a Room with Obstacles

Figure 6 presents the same speech waveform injected into the complex room. The source is located near the right wall, between two pillars. The added complexity of both the geometry and the source results in a rich wavefield, with asymmetric diffraction, localized amplification, and high-frequency interference patterns. Compared to the earlier box simulation, the presence of internal structures redistributes wave energy, resulting in uneven sound exposure across the domain.

F. Conversation Simulation with Two Sources

Figure 7 simulates a conversation composed of two consecutive speech waveforms. The first speech originates near the lower-right corner (close to the bottom pillar), and the second follows from a source near the upper-right corner. As the simulation progresses, the pressure field becomes increasingly chaotic. Reflections, diffractions, and wave superposition combine to produce nonuniform acoustic behavior, particularly in central regions of the room where wavefronts converge.

G. Snapshot of a High-Interference Moment

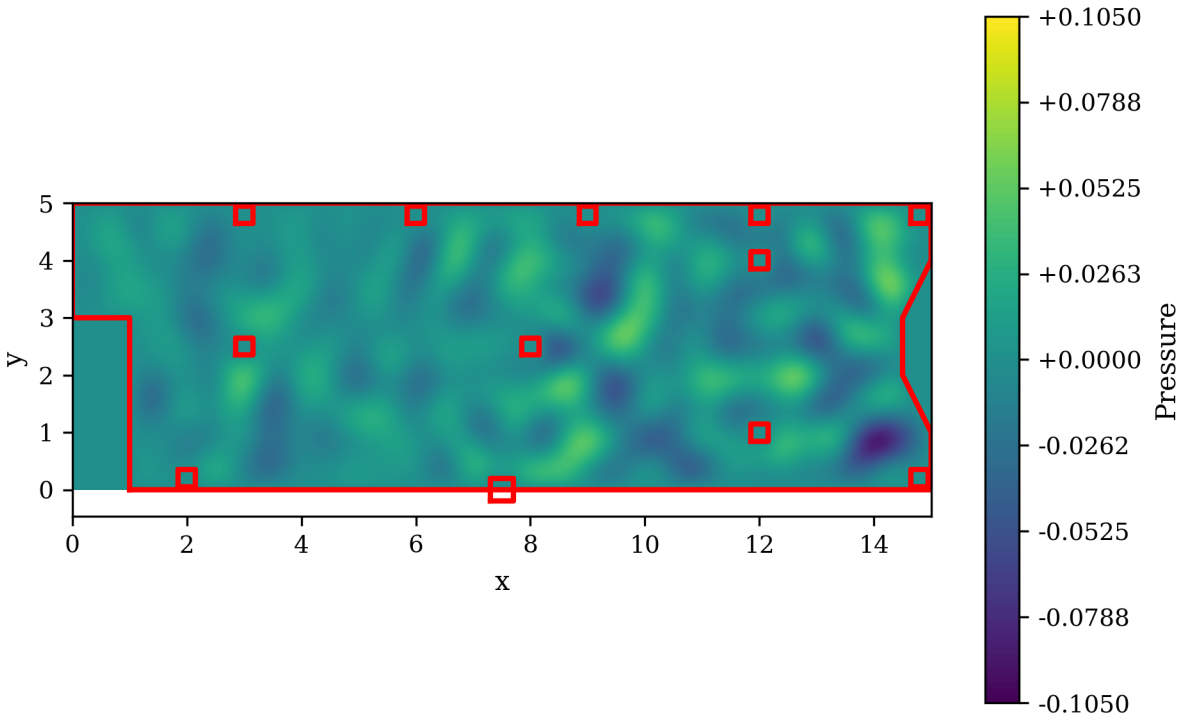

Fig. 2 Pressure field at $t = 44$ ms during the conversation simulation.

Figure 2 provides a snapshot of the pressure field at $t = 44$ ms during the conversation simulation. At this point, waves from both sources have undergone several reflections and have begun to overlap. The resulting interference

creates multiple localized zones of high pressure and deep nulls, which are indicative of transient standing waves and phase cancellation. The asymmetric layout of the pillars and walls further contributes to the irregular pressure contours. This figure illustrates how a momentary interaction between short speech bursts can produce nonuniform and amplified sound levels in certain areas of the room–offering a clear explanation for why environments like the Aero Space can become subjectively "loud" even with limited conversational activity.

VI. Conclusion

This project implemented a second-order accurate finite-difference time-domain (FDTD) scheme to simulate acoustic wave propagation in two dimensions. The numerical method was verified through a convergence study, which confirmed second-order accuracy with respect to spatial discretization, validating the solver's correctness for smooth, analytical solutions.

Once validated, the solver was used to explore the acoustic response of increasingly complex scenarios. Simulations began with a single pulse in a symmetric rectangular box, demonstrating accurate reflection behavior and conservation of wave symmetry. More intricate waveforms were then introduced, including a speech-like signal composed of three temporally offset pulses. These tests confirmed the solver's ability to handle interference, pulse accumulation, and wavefront interactions in reflective environments.

Subsequent simulations modeled wave propagation in a realistic room geometry based on the UIUC Aero Space, including internal rectangular pillars and nonuniform boundaries. In this setting, wavefronts exhibited diffraction, symmetry breaking, and complex interference patterns. A final case modeled a two-person conversation as two consecutive speech waveforms. The resulting wavefield showed substantial spatial variability and pressure amplification due to constructive interference, providing a numerical explanation for the perceptual loudness observed in reflective environments like the Aerolab.

Overall, the project demonstrates that even with modest source complexity, reflective enclosures can give rise to standing waves, pressure hotspots, and highly irregular acoustic behavior. The FDTD method proves to be a robust and accurate tool for investigating such dynamics. Future work may incorporate wall absorption models, 3D geometry extensions, or measured voice inputs to explore practical mitigation strategies for acoustic control in architectural and aerospace settings.

Appendix

A. Project Code

The respective Git repository where you can find the project code workflow published unequivocally for modularity and reproducibility.

B. Roles

1. Golemis, Shaun

18% contribution (3, 4, 5)

Wrote the final results and discussion section and verified that the explanations correctly interpreted the findings. Ensured that the results and discussion section answered the questions posed in the introduction. Evaluated the paper to be confident that it follows all instructions given by the professor.

2. Kemp, John

18% contribution (3, 4)

Helped format the paper and write part of the results section to explain figures and error graphs with help from ChatGPT to provide feedback on how to best interpret findings. Revised paper to fix grammar and formatting errors.

3. Ochs, Ben

24% contribution (2, 3, 6)

Generated the bounding box code to create the Aero Space simulation. Integrated that code into the numerical solver with the help of Josh and ChatGPT. Wrote the introduction, verified the accuracy of the mathematical formulation, and

wrote the first draft of the results and discussion.

4. Peters, Karsten

15% contribution (1, 2)

Helped brainstorm potential problems and ways to solve this chosen one. Assisted Josh with the mathematical explanations. Edited the paper before submission.

5. Veranga, Joshua

25% contribution (1, 2, 3, 4, 6)

Developed the problem and discussed with Professor Goza whether this would have a solvable solution. Described the problem, created questions, and developed the mathematical description. Developed the numerical solver and integrated the bounding box code with the help of Ben and ChatGPT. Added images of results from different tests and added the convergence test plot.

C. Figures

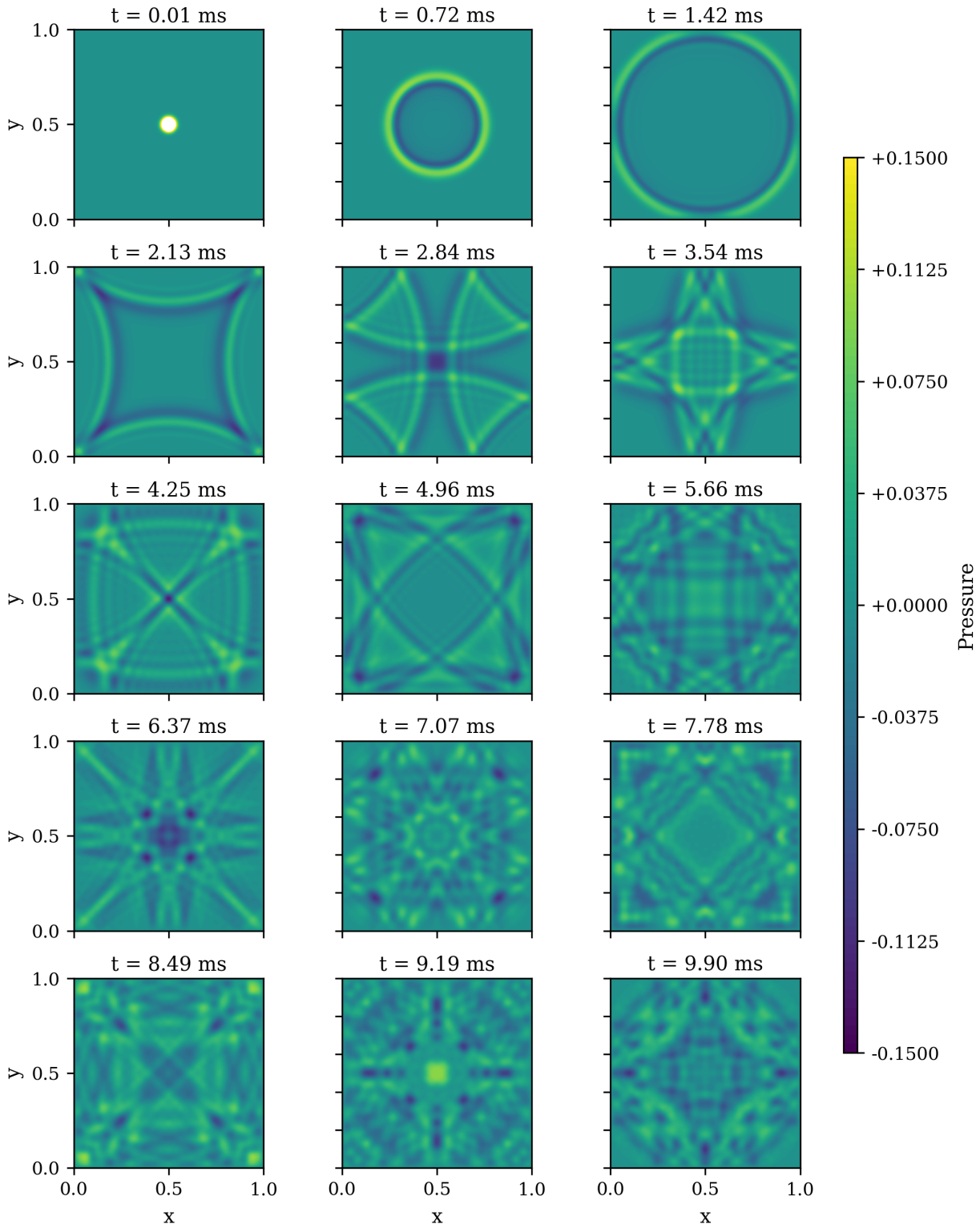

Fig. 3 Snapshots of a single acoustic pulse propagating in a rectangular box with reflective walls.

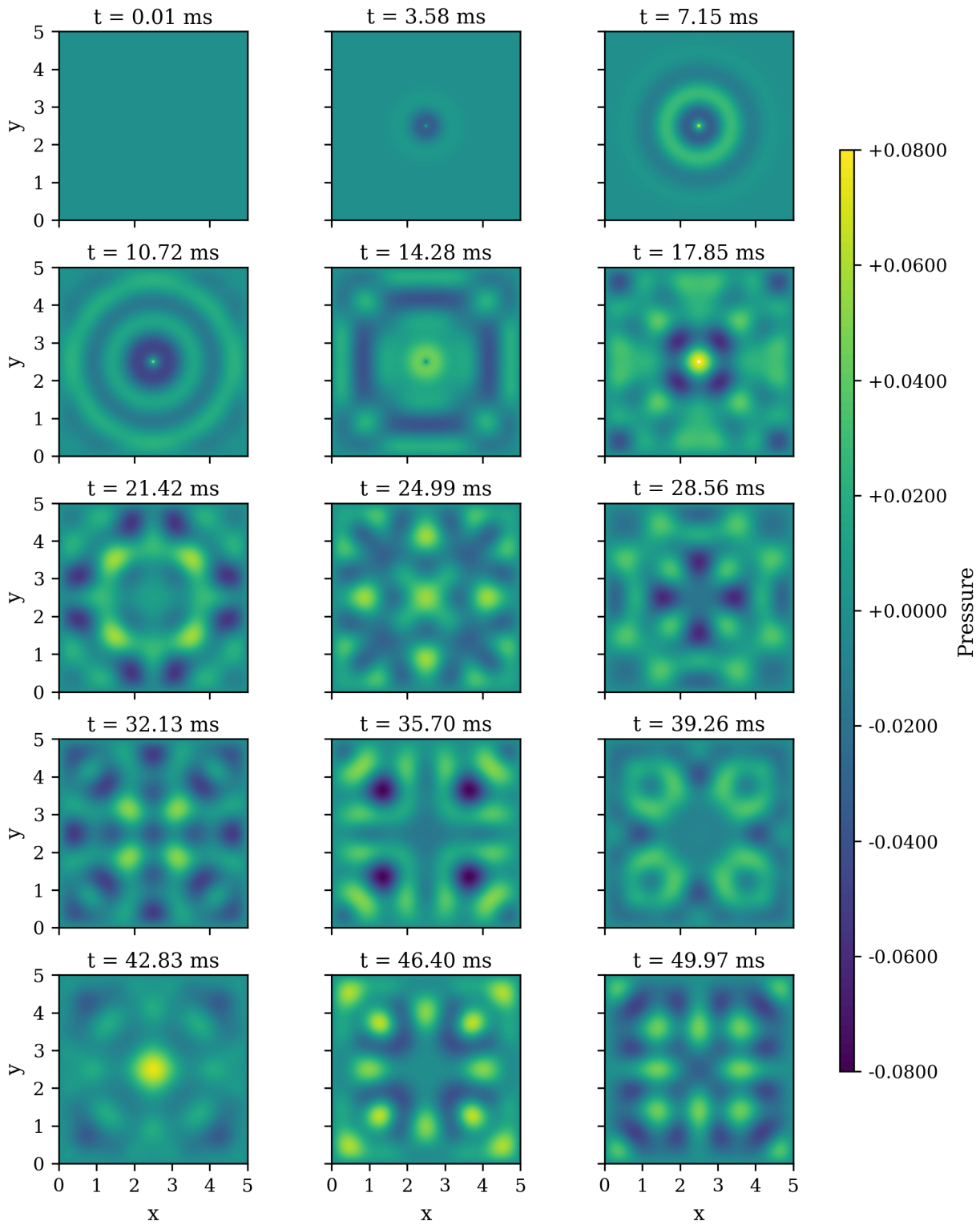

Fig. 4 Snapshots of a speech-like waveform composed of three modulated pulses ("heh - lo - there") propagating in a rectangular box.

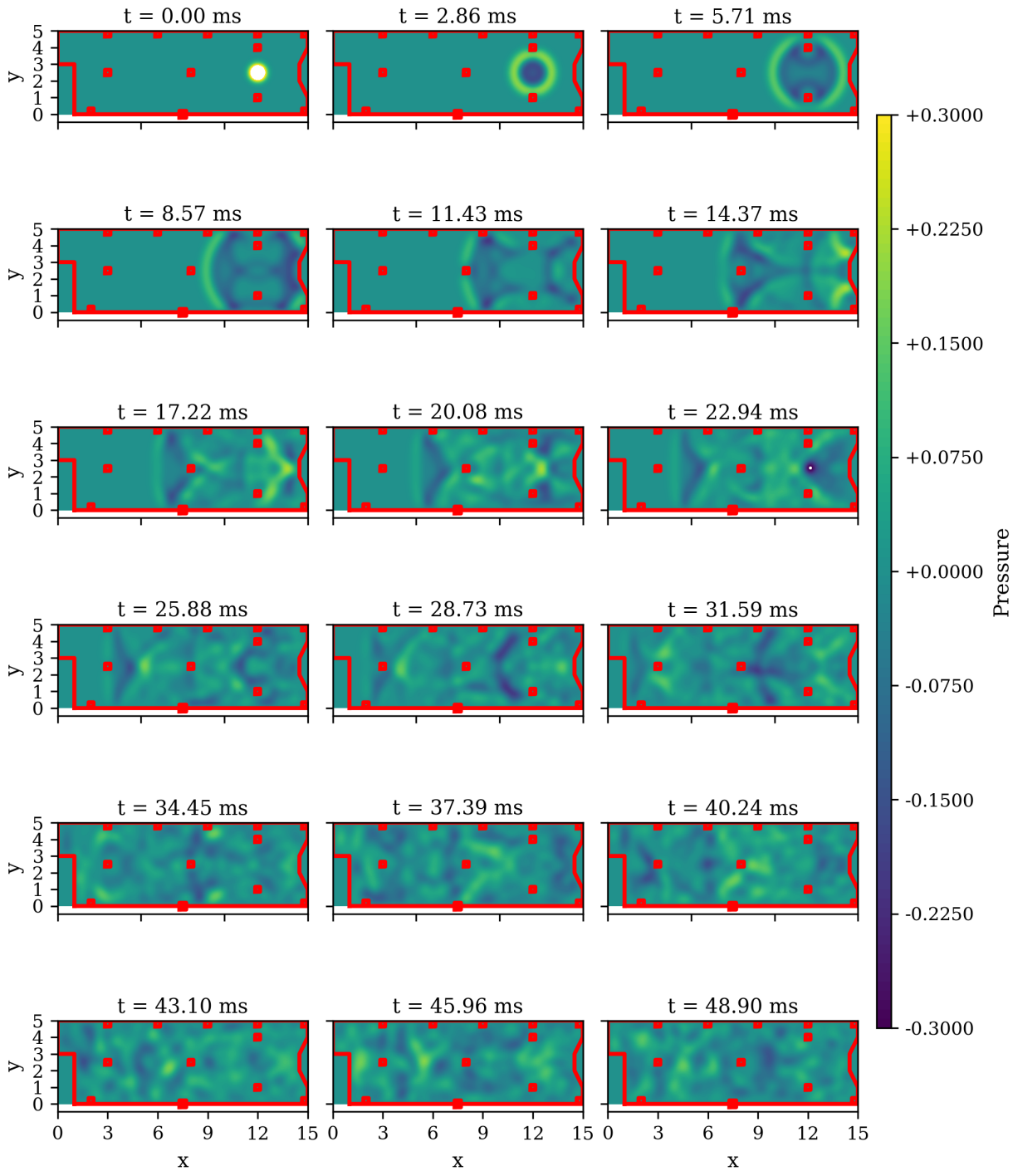

Fig. 5 Snapshots of a single pulse propagating in a realistic room geometry featuring reflective walls and rectangular pillars.

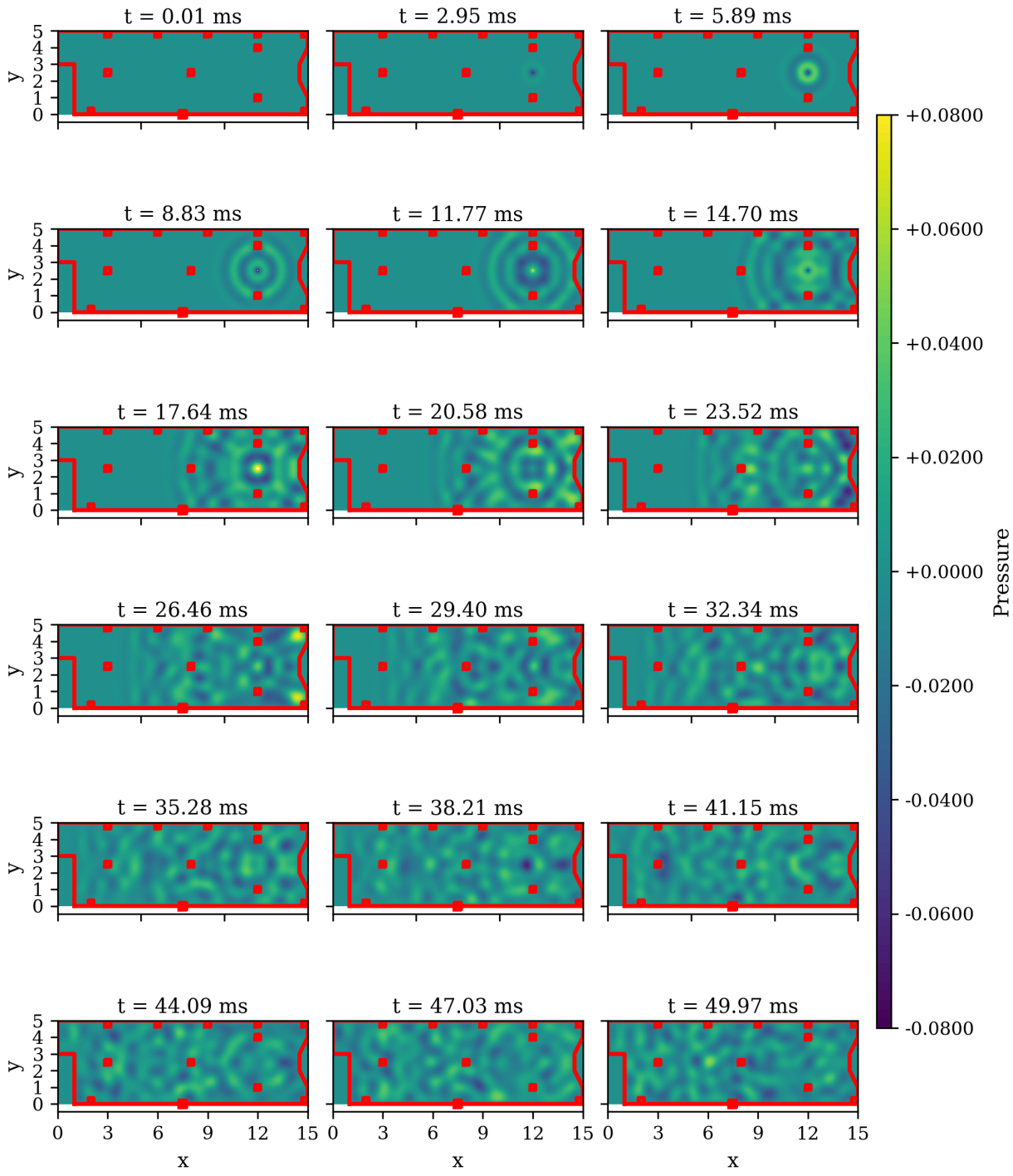

Fig. 6 Snapshots of a speech-like waveform propagating in the realistic room geometry.

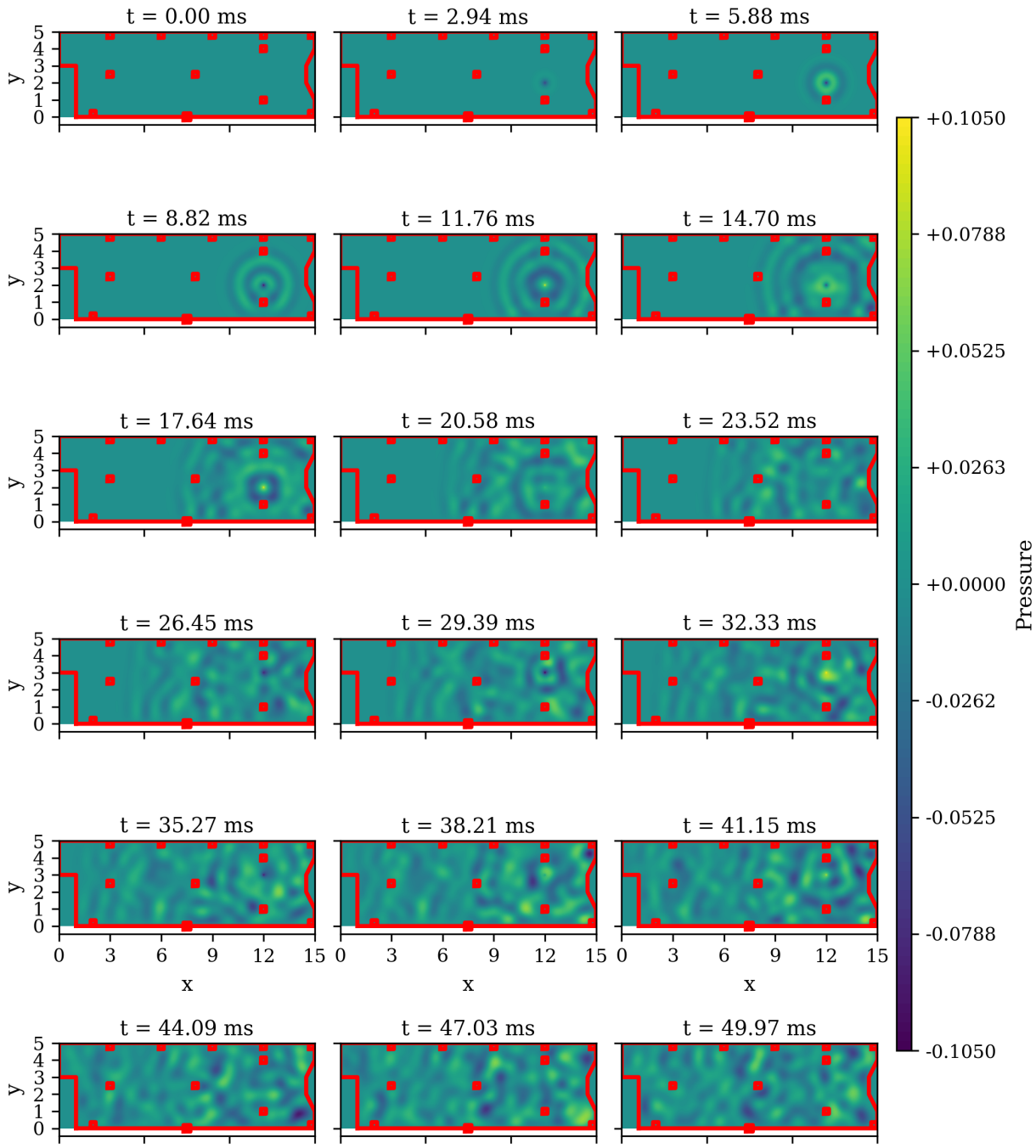

Fig. 7 Snapshots from a simulation of a two-speaker conversation, modeled as two speech bursts from different locations within the room.

Acknowledgments

We gratefully acknowledge the guidance of Professor Andres Goza and the support provided by the course teaching and course assistant staff throughout the duration of the project. Additional thanks are extended to the Department of Aerospace Engineering at the University of Illinois at Urbana-Champaign for providing the computational resources and educational framework necessary for this work.

We also acknowledge the use of OpenAI's ChatGPT as a computational assistant during this project. It was used to accelerate code development through prompt-based generation of numerical methods.

References

[1] LeVeque, R. J., *Finite Difference Methods for Ordinary and Partial Differential Equations: Steady-State and Time-Dependent Problems*, SIAM, 2007.

[2] Taflove, A., and Hagness, S. C., *Computational Electrodynamics: The Finite-Difference Time-Domain Method*, 3rd ed., Artech House, 2005.

[3] Botteldooren, D., "Finite-difference time-domain simulation of low-frequency room acoustic problems," *The Journal of the Acoustical Society of America*, Vol. 98, No. 6, 1995, pp. 3302–3308.